Plant Physiol. (1997) 115: 1319–1328

Cellular Localization of Arabidopsis Xyloglucan Endotransglycosylase-Related Proteins during Development and after Wind Stimulation[1]

Danuta M. Antosiewicz[2], Mary M. Purugganan, Diana H. Polisensky, and Janet Braam*

Department of Biochemistry and Cell Biology, Rice University, Houston, Texas 77005–1892

A gene family encoding xyloglucan endotransglycosylase (XET)-related proteins exists in Arabidopsis. *TCH4*, a member of this family, is strongly up-regulated by environmental stimuli and encodes an XET capable of modifying cell wall xyloglucans. To investigate XET localization we generated antibodies against the TCH4 carboxyl terminus. The antibodies recognized TCH4 and possibly other XET-related proteins. These data indicate that XETs accumulate in expanding cells, at the sites of intercellular airspace formation, and at the bases of leaves, cotyledons, and hypocotyls. XETs also accumulated in vascular tissue, where cell wall modifications lead to the formation of tracheary elements and sieve tubes. Thus, XETs may function in modifying cell walls to allow growth, airspace formation, the development of vasculature, and reinforcement of regions under mechanical strain. Following wind stimulation, overall XET levels appeared to decrease in the leaves of wind-stimulated plants. However, consistent with an increase in *TCH4* mRNA levels following wind, there were regions that showed increased immunoreaction, including sites around cells of the pith parenchyma, between the vascular elements, and within the epidermis. These results indicate that TCH4 may contribute to the adaptive changes in morphogenesis that occur in Arabidopsis following exposure to mechanical stimuli.

The size, shape, and arrangement of cells are the bases of plant form. The plant cell wall is a fundamental determinant of these cellular characteristics, yet the regulation of cell wall properties is not well understood. Recently, XETs have been discovered (Smith and Fry, 1991; Farkas et al., 1992; Fry et al., 1992; Nishitani and Tominaga, 1992; Fanutti et al., 1993), and these enzymes are proposed to modify the extensibility and strength of plant cell walls (Fry, 1989; Smith and Fry, 1991; Fry et al., 1992; Passioura and Fry, 1992; Talbott and Ray, 1992). The substrate for XETs is xyloglucan, the major hemicellulose of the growing primary dicotyledonous cell wall, which is thought to form cross-links between cellulose microfibrils (Hayashi et al., 1987, 1994a, 1994b; Hayashi, 1989; Fry, 1989; McCann et al., 1990; Passioura and Fry, 1992; Carpita and Gibeaut, 1993; McCann and Roberts, 1994). The breaking and joining of the xyloglucan polymers carried out by XETs may contribute to the incorporation of new xyloglucan into the growing cell wall (Edelmann and Fry, 1992; Nishitani and Tominaga, 1992; Talbott and Ray, 1992; Nishitani, 1995; Xu et al., 1996) or a rearrangement of xyloglucan chains during cell expansion (Fry, 1989; Smith and Fry, 1991; Fry et al., 1992).

Arabidopsis *TCH4*, a mechanostimulus-inducible gene (Braam and Davis, 1990; Xu et al., 1995; Braam et al., 1996; Xu et al., 1996), encodes an XET enzyme that shares 41 to 65% identity in amino acid sequence to other known XETs (Xu et al., 1995). Recombinant TCH4 protein produced in *Escherichia coli* has been shown to be active specifically against xyloglucan substrates with an unexpected preference for a nonfucosylated xyloglucan oligosaccharide (Purugganan et al., 1997). In addition, TCH4 is most active at pH 6.0 to 6.5, and its activity is remarkably cold tolerant with a temperature optimum of 12 to 18°C (Purugganan et al., 1997).

An extensive gene family in which the members share sequence similarities with *TCH4* has been identified in Arabidopsis (Xu et al., 1996). The members of this family have been called *XTRs* for XET- related and include *Meri-5* (Medford et al., 1991), *EXT* (Okazawa et al., 1993), and at least five other Arabidopsis genes that share 37 to 84% amino acid identity (Xu et al., 1996). Expression of the *XTRs* is differentially regulated by environmental and hormonal stimuli, and the magnitude and kinetics of regulation are distinct for the different genes (Xu et al., 1996). The *XTRs* may also be spatially and temporally regulated in expression during development (Xu et al., 1996).

In addition to endogenous cues, external stimuli can lead to dramatic alterations in plant development. Morphogenetic changes often occur in plants as a response to stressful environmental conditions; these alterations can result in phenotypes better adapted to the particular environment. For example, plants exposed to wind generally develop to be shorter and stockier than plants grown under sheltered conditions (Biddington, 1986; Jaffe and Forbes, 1993; Mitchell and Myers, 1995). Because the cell wall influences plant cell growth, modifications of the wall are most likely crit-

[1] This research was supported by a National Science Foundation grant (no. IBN-9418750) to J.B. M.M.P. was supported in part by a National Institutes of Health training grant (no. GM07833) and a Lodieska Stockbridge Vaughan Fellowship.

[2] Present address: University of Warsaw, Institute of Plant Experimental Biology, Department of Morphogenesis, Environmental Plant Pollution Laboratory, Krakowskie Przedmiescie 26/28, 00–927 Warsaw, Poland.

* Corresponding author; e-mail braam@bioc.rice.edu; fax 1–713–285–5154.

Abbreviations: CaMV, cauliflower mosaic virus; XET, xyloglucan endotransglycosylase.

ical for these morphogenetic responses to the environment. The *TCH4* gene is strongly and rapidly up-regulated by environmental stimuli and encodes an XET; therefore, *TCH4* may play a role not only in the control of normal plant development but also in eliciting environmentally induced morphogenetic changes.

To identify where and when XETs may function during plant development, we determined the tissue- and cell-specific localization pattern using antibodies generated against TCH4. Based on these results, we discuss the possible physiological functions of XETs in Arabidopsis morphogenesis.

MATERIALS AND METHODS

Plant Material and Treatments

Arabidopsis thaliana plants, ecotype Columbia, were cultivated in a plant growth room under continuous light at 24°C in 65 to 75% RH. Plants grown in soil were used for shoot material. For growth of sterile roots, plants were grown in Petri plates with 0.5× Murashige and Skoog salts (Sigma), 1× Gamborg's vitamins (Sigma), and 1% Suc, pH 5.7.

Touch treatments were done by gently touching the rosette leaves and bending the plants back and forth approximately 10 times. Plants were harvested 90 min after stimulation. For continuous wind stimulation, 6-d-old seedlings were gently blown by a fan to result in leaf movement. The wind treatment was continued for 4 d.

To assess the specificity of the anti-TCH4 antisera, we used transgenic plants that have altered levels of accumulation of TCH4. The generation and characterization of these transgenic plants will be more fully detailed in a future manuscript (M.M. Purugganan and J. Braam, unpublished results). Briefly, antisense plants harbor a 989-bp *Hin*dIII fragment of *TCH4* genomic sequence extending from −721 to +268 (where +1 is the transcriptional start site). This fragment is cloned in the antisense orientation between the CaMV 35S promoter and the nopaline synthase terminator, derived from the pBi221 vector (Clontech, Palo Alto, CA), such that the complementary strand to the *TCH4* mRNA is transcribed. Plants overexpressing *TCH4* harbor between the CaMV 35S promoter and the nopaline synthase terminator the 853-bp fragment of *TCH4* cDNA, such that the entire TCH4 protein-coding sequence is transcribed (encoding 284 amino acids).

Antibody Production and Immunoblotting

A 366-bp DNA fragment encoding the last 122 amino acids of the carboxyl-terminal region of TCH4 was ligated into pET21 (Novagen, Madison, WI). The resulting plasmid, pMP2, was transformed into BL21(DE3)pLysS cells (Novagen). The manufacturer's directions were followed for the production of the target protein and the isolation of the crude insoluble protein fraction, which contained the TCH4 polypeptide. The insoluble proteins were separated on a 12% SDS-polyacrylamide gel. After electrophoresis the gel was stained with aqueous 0.05% Coomassie brilliant blue R-250 for 10 min and washed with numerous changes of water over several hours. When the band corresponding to TCH4 was visible, it was excised from the gel, placed on dry ice, and sent to Cocalico Biologicals (Reamstown, PA) for inoculation of rabbits. Serum was stored at −80°C. The preimmune and anti-TCH4 antisera were affinity purified by binding to TCH4 antigen-containing Aminolink TM columns (Pierce) generated and used according to manufacturer's specifications.

Fresh shoot tissue from unstimulated 2-week-old plants was ground using a pestle and mortar, together with 0.5 M NaCl and a sprinkling of white quartz sand (−50 +70 mesh, Sigma). The homogenate was centrifuged at 12,000*g* for 5 min at 4°C. The supernatant was stored at −20°C.

Laemmli's 5× sample buffer (10% SDS, 50% glycerol, 0.3 M Tris-HCl, pH 6.8, 0.5 M DTT, and 0.005% bromphenol blue) was added to approximately 80 μg of protein to a final concentration of 1× and boiled for 10 min immediately before loading onto a 10% resolving, 5% stacking SDS-polyacrylamide gel for electrophoresis.

Tris-Gly buffer (0.025 M Tris-HCl, pH 8.3, 0.192 M Gly, and 20% methanol) was used to effect transfer of protein to nitrocellulose using the Mini Transblot System (Bio-Rad). The blot was dried at room temperature.

Free binding sites were blocked with 0.15% Tween 20 (Boehringer Mannheim) in 1× PBS and probed with affinity-purified anti-TCH4 antibody at 2 μg/mL in 0.15 M NaCl, 0.01 M Tris-HCl, pH 7.5, 0.1% Tween 20, 1% nonfat milk, and 0.02% sodium azide. Excess antibody was removed with extensive washing in 0.05% Tween 20 (Fisher Scientific) in 1× PBS.

Secondary antibody, donkey anti-rabbit IgG conjugated with horseradish peroxidase (Amersham) at 1:5000 (v/v) in 0.15 M NaCl, 0.01 M Tris-HCl, pH 7.5, 0.1% Tween 20, 1% nonfat milk, and 0.003% thimerosol (Sigma) was applied and then extensively washed as above. Antigen/antibody complexes were visualized using the chemiluminescence Supersignal CL-HRP Substrate System (Pierce).

Immunocytochemistry

For the majority of experiments, 10-d-old seedlings were analyzed. However, for examination of mature leaves, the first pair of leaves of 18-d-old plants was used. Small pieces of plant material (about 2–4 mm^2, 0.5–2 mm^3) were fixed in a solution of 4% paraformaldehyde and 0.5% glutaraldehyde in 0.05 M sodium phosphate buffer, pH 7.3, for 2 h at room temperature and then continued overnight (12–14 h) at 4°C. Samples were washed in 0.05 M sodium phosphate buffer and dehydrated in a graded series of ethanol. Tissues were then embedded in Steedman's wax (Norenburg and Barrett, 1987). Sections (6–14 μm) were affixed to slides precoated with high-molecular-weight poly-L-Lys.

Sections were rehydrated in ethanol and then incubated in PBS overnight (approximately 12 h). One hour of incubation in PBS with 2% dry milk, 0.015 M NaCl, and 0.1 M NH_4Cl was used to block nonspecific binding. Affinity-purified primary antibody (6 μg/mL) in blocking solution was applied to sections for 2 h at room temperature followed by an overnight incubation at 4°C. The tissue was

then washed for 10 min in blocking solution and then washed twice for 10 min in 0.1 M Tris-HCl, pH 7.5, 0.15 M NaCl, 0.5% Tween 20, and 5% dry nonfat milk (solution A). Secondary antibody (alkaline phosphatase-conjugated goat anti-rabbit, Sigma) was diluted 1:100 with solution A and applied for 1 h at room temperature. Sections were rinsed for 10 min in solution A and then washed twice for 5 min in solution A lacking dry milk. Substrate (200 μL of 0.165 mg/mL nitroblue tetrazolium and 0.08 mg/mL 5-bromo-4-chloro-3-indolyl phosphate in 0.1 M NaCl, 0.005 M $MgCl_2$, and 0.1 M Tris-HCl, pH 9.5) was incubated with the sections for 2 h. The reaction was stopped by washing in 0.01 M Tris-HCl, pH 8.0, and 0.001 M EDTA. Sections were then dehydrated and mounted with Permount (Fisher Scientific) and photographed with a Photo Microscope III (Zeiss). Photographs showing reproducible staining patterns were chosen for the figures. Controls consisting of omission of primary antibody, omission of secondary antibody, omission of both antibodies, and use of preimmune rabbit serum gave little or no background staining. To examine the structure of leaves, sections were stained with Harris hematoxylin (Fisher Scientific).

RESULTS

Specificity of Affinity-Purified TCH4 Antiserum

Rabbit antisera were generated against the carboxyl-terminal region of TCH4. After affinity purification, the antibodies recognized a single band on western blots of the predicted size of TCH4 (33.4 kD), as shown in Figure 1. Under similar conditions preimmune antibodies subjected to affinity purification showed no detectable immunoreaction (data not shown). To verify that the band detected by the antisera is TCH4, we compared the pattern and intensity of the immunoreaction of proteins isolated from wild-type plants (Fig. 1, lane 2) with proteins from transgenic plants that underproduce TCH4 protein as a consequence of expression of a *TCH4* antisense gene (Fig. 1, lane 1), and transgenic plants that overproduce TCH4, as a result of harboring a constitutively active *TCH4* gene (Fig. 1, lane 3).

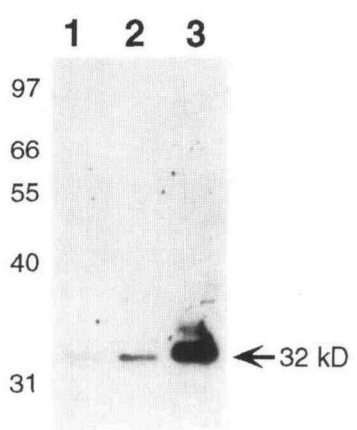

Figure 1. Total proteins were analyzed from *TCH4* antisense (lane 1), wild-type (lane 2), and *TCH4*-overexpressing (lane 3) plants by immunoblotting using affinity-purified anti-TCH4 antibody.

Plants harboring a *TCH4* transcription unit downstream of the relatively constitutive and strong CaMV 35S promoter have dramatically higher levels of antigenically reactive protein (Fig. 1, lane 3), demonstrating that the antibodies are clearly capable of binding TCH4.

The faint band seen above the major band in Figure 1, lane 3, was seen only in protein extracts from plants overproducing TCH4 and, therefore, is most likely a modified form of the TCH4 protein that is detectable when large amounts of TCH4 are generated. The production of antisense transcripts complementary to the first 268 bases of the *TCH4* mRNA results in a decrease in immunoreactivity (Fig. 1, lane 1), providing evidence for specificity of the antibodies. A band was still detectable in lane 1, however, suggesting either that some TCH4 protein remains in these antisense plants or that the antisera are also capable of recognizing an XTR protein or proteins closely related to and of the same apparent molecular mass as TCH4. Because of the complication of the presence of an extensive *TCH4*-related gene family in Arabidopsis and the possibility for cross-reactivity of the antisera, we interpret the data presented here as an analysis of the pattern of the TCH4 XET and possibly other Arabidopsis XETs that are antigenically related to TCH4.

XET Accumulation in Epicotyls, Hypocotyls, and Cotyledons

In 10-d-old Arabidopsis epicotyls XETs were found evenly distributed over the apical meristem (Fig. 2A), as evidenced by the light-blue staining (compare with Fig. 2D for control background staining). Cells of leaf primordia also contained the antigen; however, the immunostaining was uneven in that there were files of cells that had significantly higher levels of detectable XETs (Fig. 2A). Although limited to only a few cells of the pith parenchyma, XETs were found at high levels at cellular junctions or intercellular regions between cells (Fig. 2, A and B) and were also found in procambial strands (Fig. 2C). As expected for enzymes that modify wall components, the XETs appeared to accumulate at cellular boundaries, most likely within the wall itself. Occasionally, immunostaining appeared to be present around nuclei, as in Figure 2C. This staining was most likely due to immunoreactions with nascent protein being produced in the perinuclear ER. The staining patterns detected were specific for the XET antigen because, as shown in Figure 2D, the preimmune serum showed no significant immunoreaction.

XETs were restricted to the vascular tissue of the distal hypocotyl (Fig. 2E) and were found preferentially in immature, differentiating xylem vessels and between vessels, most likely within the middle lamella or intercellular spaces (Fig. 2F). Single cells within the phloem also showed intense immunolabeling (Fig. 2F). Within the central cylinder of the base of the hypocotyl, XETs localized preferentially to the xylem cambium derivatives that differentiate into secondary xylem (Fig. 2G).

Within mature cotyledon blades (Fig. 2H) and the distal regions of cotyledon petioles (data not shown), XETs were found only in the vascular bundles. The staining was

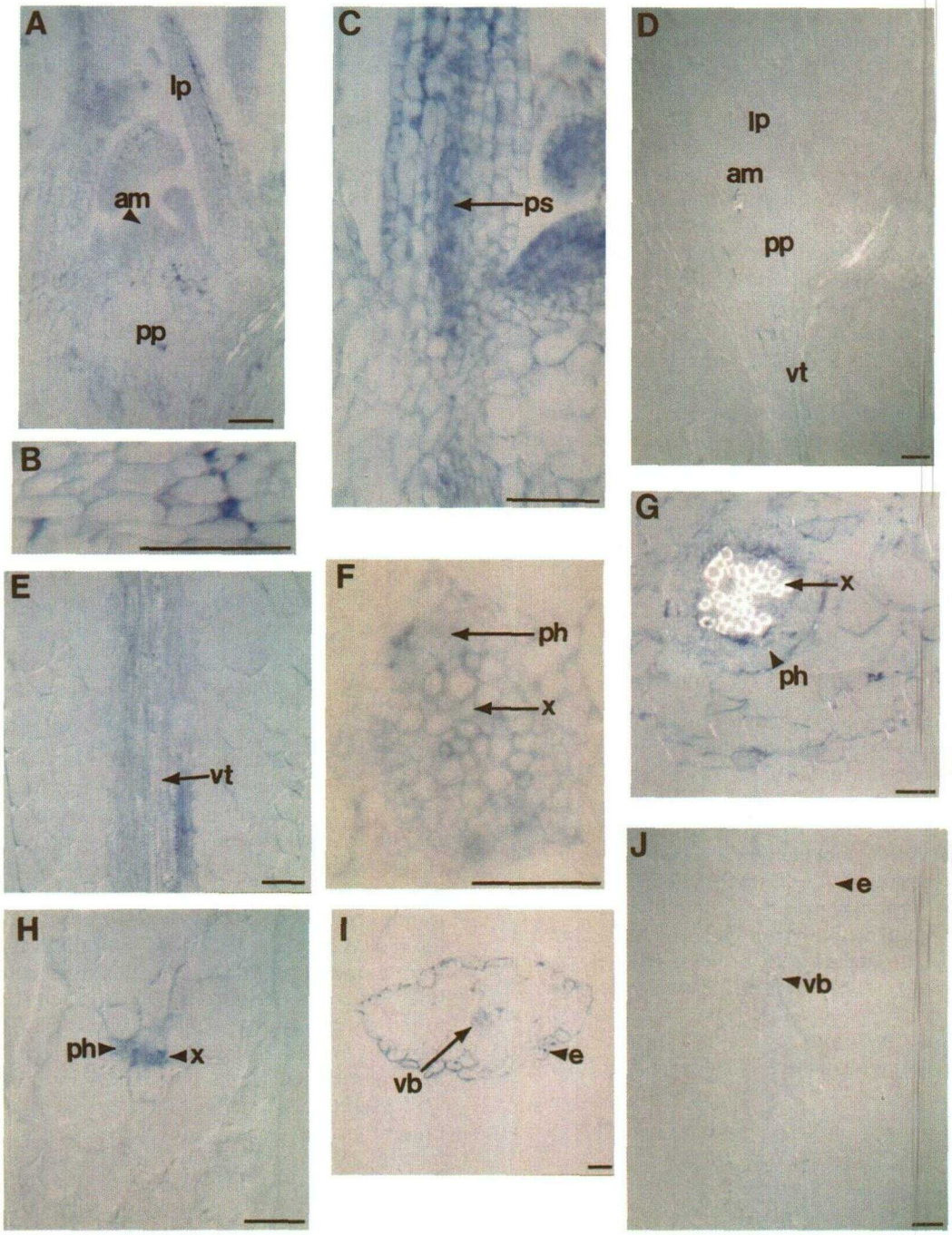

Figure 2. Blue staining indicates the presence of XETs. Sections were photographed with Nomarski optics, except for F, for which bright-field optics were utilized. A, Shoot apex (longitudinal section). XETs were in the shoot apical meristem, leaf primordia, and between individual pith parenchyma cells. B, Pith parenchyma (longitudinal section through the epicotyl). XETs were found between individual cells. C, Leaf primordium (longitudinal section through the base). XETs accumulated primarily in the procambium. D, Shoot apex (longitudinal section). Preimmune serum showed no immunoreaction. E, Upper part of the hypocotyl (longitudinal section). XETs were in the vascular tissue. F, Vascular tissue of the hypocotyl (transection). XETs accumulated inside developing, immature vessels and, to a lesser extent, between vessels. Immunostaining in the phloem is less strong. G, Base of the hypocotyl (transection). XETs were in all tissues but were most abundant in differentiating xylem elements. H, Cotyledon blade (transection). XETs were restricted to the vascular bundle. I, Base of the cotyledon petiole (transection). XETs were abundant in the vascular bundle and in the epidermis. J, Cotyledon blade (transection). Preimmune serum showed no immunoreaction. am, Apical meristem; e, epidermis; lp, leaf primordium; ph, phloem; pp, pith parenchyma; ps, procambium strand; v, vessel; vb, vascular bundle; vt, vascular tissue; and x, xylem. Bars = 100 μm.

clearly due to the localized presence of antigen because the preimmune sera showed no reaction (Fig. 2J). XETs were also very abundant in the epidermis at the base of the cotyledon petiole (Fig. 2I).

XET Localization during Leaf Development

In small leaf primordia approximately 60 μm in height, XETs were found uniformly distributed and at moderate levels in meristematic cells that were nonvacuolated or that contained small vacuoles (Fig. 3B). The intensity of immunostaining gradually decreased with increased vacuolization (Fig. 3B), with highly vacuolated, enlarged cells in the midrib area of developing leaf blades that lacked significant levels of XET protein (Fig. 3E). In older primordia striking XET accumulation was seen in a subset of expanding cells (Fig. 3, C and D). This strong labeling is unusual in that it was not uniform within or around specific cells but instead was confined to either the region between two rows of cells (Fig. 3C) or corners where multiple cells come into contact (Fig. 3D). This staining pattern may reflect a role for XET proteins in modifying cell-cell contacts.

During leaf blade formation moderate levels of XETs remained in the small, nonvacuolated cells, and the intense immunostaining at cellular junctions was still prominent (Fig. 3, E and F). At this developmental stage, XETs are abundant between the first and second layer of meristematic cells that differentiate into spongy parenchyma. These rows of cells, as shown in developing leaf blade tissue stained with hematoxylin (Fig. 3G), were in the early stages of intercellular airspace formation. Later in leaf blade development, when the palisade parenchyma cells are forming intercellular spaces, XETs were highly abundant between the rows of these cell types (Fig. 3H). In addition, differentiating spongy parenchyma cells in expanding margins of leaf blades also contained high levels of XET antigen at cellular junctions (Fig. 3, H and I). The moderate levels of XETs throughout the rest of the leaf were lost, because differentiation is almost complete (Fig. 3I). XETs were sometimes also detected between fully vacuolated cells, as shown in the developing primordium in Figure 3J. Consistently, XETs were present in procambial strands and in developing vascular tissue (Fig. 3, C–E and H–J). Figure 3K shows background staining obtained when preimmune antibody was used.

Mature leaves show an XET-localization pattern similar to that of cotyledons. XETs were found in both the vascular bundle and epidermis at the base of the leaf petiole (Fig. 3L) but were restricted primarily to the xylem within the leaf blade (Fig. 3M). There was also reproducible, dramatic XET labeling within a single parenchymatic cell, which is located near the phloem part of some vascular bundles (Fig. 3M).

XET Distribution in Developing Roots

At the primary root apex, XETs were localized to the proximal stories of columella cells and were absent from the meristematic zone (Fig. 4A). Further proximally, all cell types of the elongation zone accumulated XETs (Fig. 4, A and B). In more mature regions of the root, XETs were concentrated primarily within the vascular tissue, with some protein seen in certain regions of the epidermis (Fig. 4C). Pericycle cells also showed some immunostaining, and the intensity of this staining increased significantly in actively dividing pericycle cells that give rise to lateral root primordia (Fig. 4D).

In regions of secondary growth, XETs were restricted to immature xylem vessels and parenchyma cells associated with mature xylem (Fig. 4E); minimal immunostaining was detected between mature xylem vessels (Fig. 4E). Isolated cells within the secondary phloem also showed moderate levels of XETs (Fig. 4E). Figure 4F shows the lack of immunostaining detected when preimmune antibodies were used.

Alterations in the Pattern of XET Accumulation in Mechanically Stimulated Plants

Expression of the *TCH4* gene is dramatically upregulated in response to mechanical stimuli such as touch or wind (Braam and Davis, 1990). To determine the effects of such stimuli on XET localization, we examined the pattern of XET accumulation in plants subjected to either a single-touch stimulation or to 4 d of continuous wind. For these two experimental conditions, similar alterations in XET localization were observed; however, the changes following a single touch were less pronounced (data not shown). Figure 5A illustrates that after continuous wind stimulation the levels of XET frequently increased in the epicotyl pith parenchyma. Surprisingly, there was a significant decrease in XET levels in leaf primordia (compare with Fig. 2A). In developing leaves both the intensity and frequency of XET immunostaining at cellular junctions were considerably reduced (compare Fig. 5, A–C, with Fig. 3, C–F and H). Other changes in XET localization following mechanical stimulation were seen within the hypocotyl. XETs appeared within the epidermis (Fig. 5D) of the hypocotyl base where they are absent in unstimulated plants, and XET levels increased significantly between vessels (Fig. 5E).

DISCUSSION

We have shown that the TCH4 XET and possibly closely related proteins accumulate in specific cells during development and that this pattern is altered by mechanical stimulation. These data provide insight into the sites of action and possible functions of the Arabidopsis XETs.

One of the prominent ideas for a physiological function for XETs is that these enzymes perform cell wall modifications required for the process of cell expansion, either by causing cell wall loosening (Fry, 1989; Smith and Fry, 1991; Fry et al., 1992) or by incorporating xyloglucan into extending walls to prevent thinning and weakening of the wall (Edelmann and Fry, 1992; Nishitani and Tominaga, 1992; Talbott and Ray, 1992; Nishitani, 1995; Braam et al., 1996; Xu et al., 1996). Consistent with this idea, XET activity levels have been found to correlate with growth rates (Fry et al., 1992; Hetherington and Fry, 1993; Pritchard et al.,

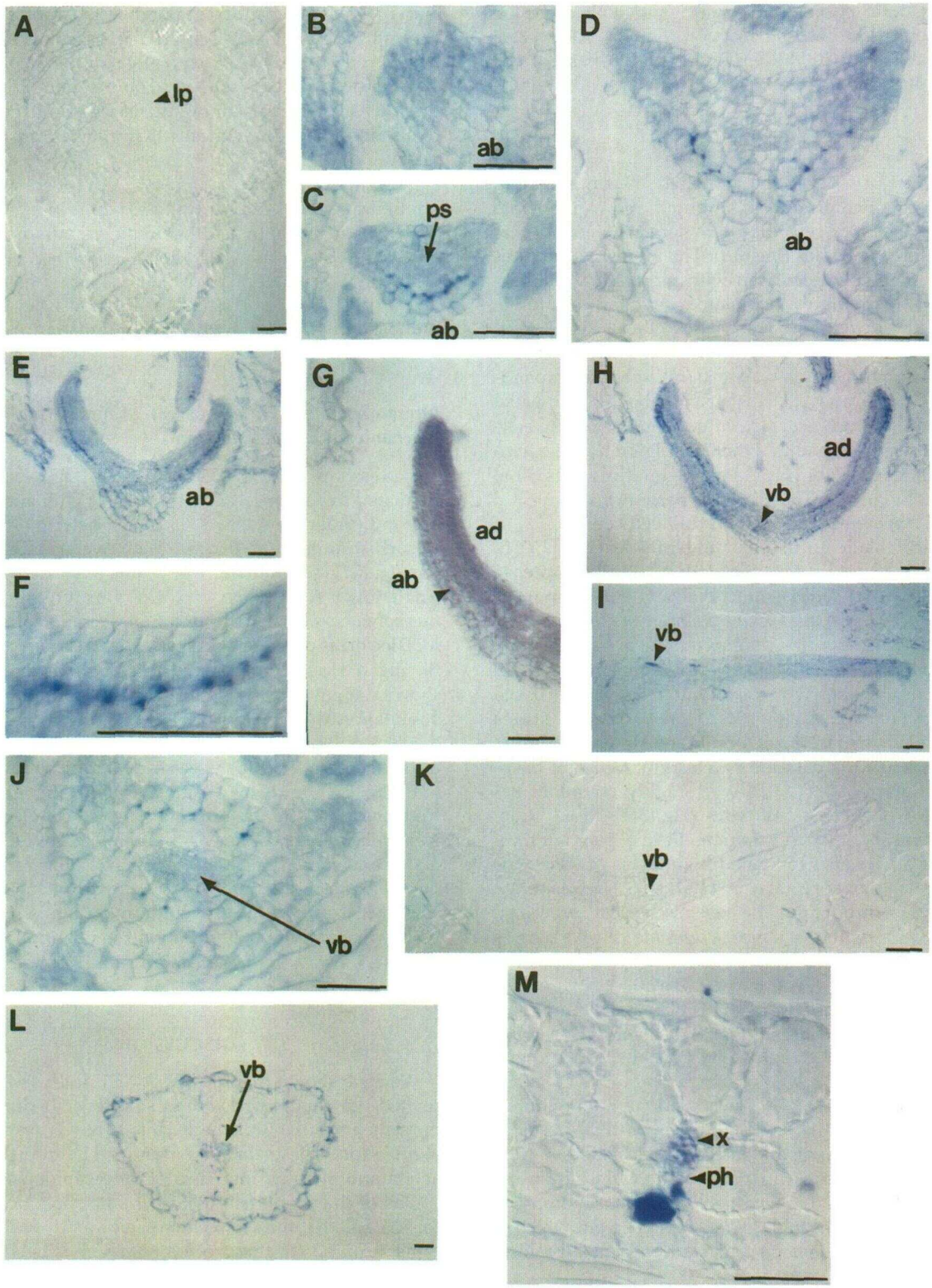

Figure 3. Blue staining indicates the presence of XETs; sections were photographed with Nomarski optics. A, Leaf primordia (transection through the base). Preimmune serum showed no immunoreaction. B, Young leaf primordium approximately 60 μm in height (transection through the base). Moderate, uniform levels of XETs were found in meristematic cells. C, Young leaf primordium of approximately 130 μm in height (transection through the middle). On the abaxial side, XETs were very abundant between two rows of cells in the early stages of vacuolization. D, Leaf primordium approximately 560 μm in height (transection through the middle). On the abaxial side, XETs were very abundant between two rows of vacuolating

(Legend continues on facing page.)

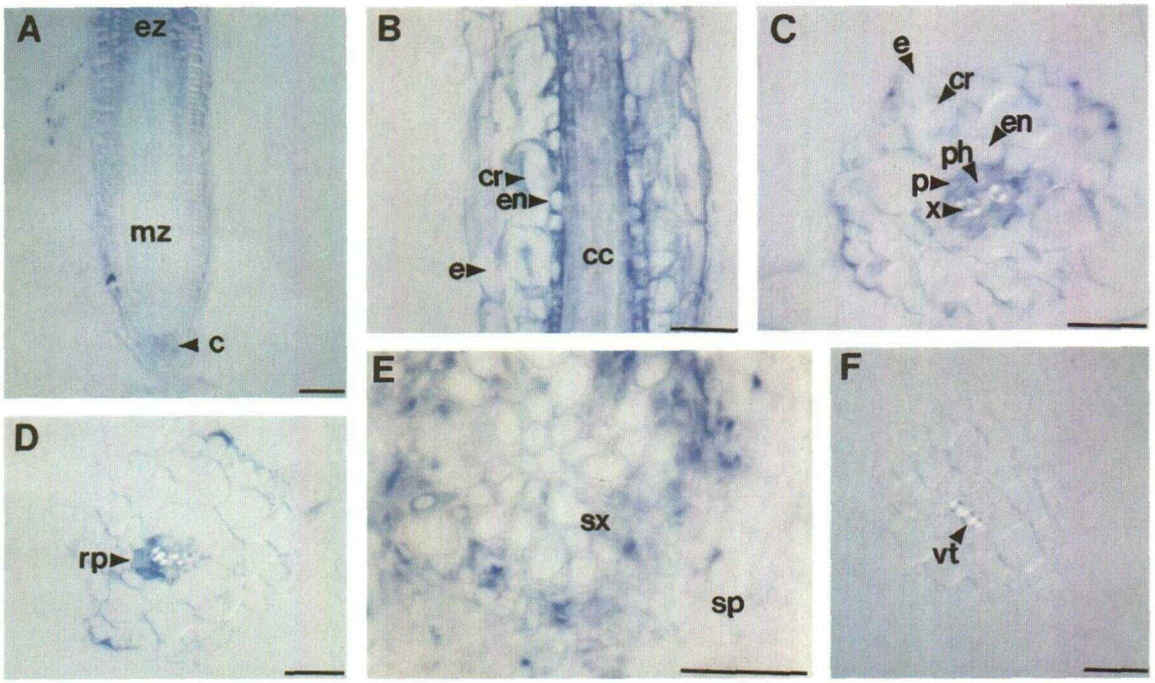

Figure 4. Blue staining indicates the presence of XETs; sections were photographed with Nomarski optics for A to D and F. Bright-field optics were used for E. A, Root tip (longitudinal section). XETs were in the columella and in the elongation zone. B, Transition from the elongation to the differentiation zone (longitudinal section). XETs accumulated in all differentiating meristematic cells. C, Primary root (transection). XETs were within the vascular tissue and pericycle. D, Lateral root formation (transection through the median part of newly initiated root primordium). Lateral root primordium was intensely immunostained. XETs were also in the vascular tissue. E, Secondary growth of the main root (transection). XETs were in the differentiating vascular elements and in xylem parenchyma cells. Minimal immunostaining was detected between xylem vessels. F, Primary root (transection). Preimmune serum showed no immunoreaction. c, Columella; cc, central cylinder; cr, cortex; e, epidermis; en, endodermis; ez, elongation zone; mz, meristematic zone; p, pericycle; ph, phloem; rp, root primordium; sp, secondary phloem; sx, secondary xylem; vt, vascular tissue; x, xylem. Bars = 100 μm.

1993; Potter and Fry, 1994; Xu et al., 1995). In addition, brassinosteroid and auxin, two growth-promoting hormones, enhance expression of several *XET*-related genes (Zurek and Clouse, 1994; Xu et al., 1995, 1996) Here we report that Arabidopsis XETs are found in several cell types that are beginning to expand. Meristematic cells of the shoot apex (Fig. 2A) and leaf primordia (Figs. 2A and 3, B and C) and cells that begin to elongate in the root (Fig. 4, A and B) all accumulate moderate levels of XETs. These data are therefore consistent with a possible role for Arabidopsis XETs in wall modifications that take place during cell expansion.

Figure 3. (Legend continued from facing page.)
cells, especially where the cells meet at the corners. E, Young leaf blade (transection). XETs were absent from highly vacuolated cells on the abaxial part of the midrib area. XETs accumulated between two cell layers of vacuolating meristematic cells that will differentiate into spongy parenchyma and form intercellular spaces. F, Developing leaf blade (transection). XETs were most abundant between cells and preferentially where they are in contact at their corners. G, Young leaf blade (successive transection of that shown in E) stained with hematoxylin. Two cell layers are differentiating into spongy parenchyma on the abaxial part of the leaf; these cells began to vacuolate and to form intercellular spaces between the cell layers (arrowhead). Meristematic cells on the adaxial part differentiated into palisade parenchyma and began to vacuolate later. H, Advanced developing leaf blade (transection). Increased levels of XETs were present between differentiating spongy parenchyma cells only at the abaxial part of the leaf margin and between two layers of differentiating palisade parenchyma cells along the adaxial part of the leaf. I, Leaf blade close to maturation (transection). Uniform, moderate levels of XETs were in meristematic cells. Strong XET immunostaining was seen only between cell layers at the margin, where the youngest cells enter into the composition of the leaf blade. XETs were absent from vacuolated cells of the central region of the blade with the exception of the vascular tissue. J, Older primordium (transection through the proximal region). XETs were abundant between vacuolated cells. K, Young leaf blade (transection). Preimmune serum showed no immunoreaction. L, Base of the petiole (transection). XETs were restricted primarily to the vascular bundle and epidermis. M, Mature leaf blade (transection). XETs were in the vascular bundle, primarily in the xylem. A striking level of XETs was seen in the single parenchyma cell close to the phloem. ab, Abaxial part of the developing leaf; ad, adaxial part of the developing leaf; lp, leaf primordium; ph, phloem; ps, procambium strand; vb, vascular bundle; and x, xylem. Bars = 100 μm.

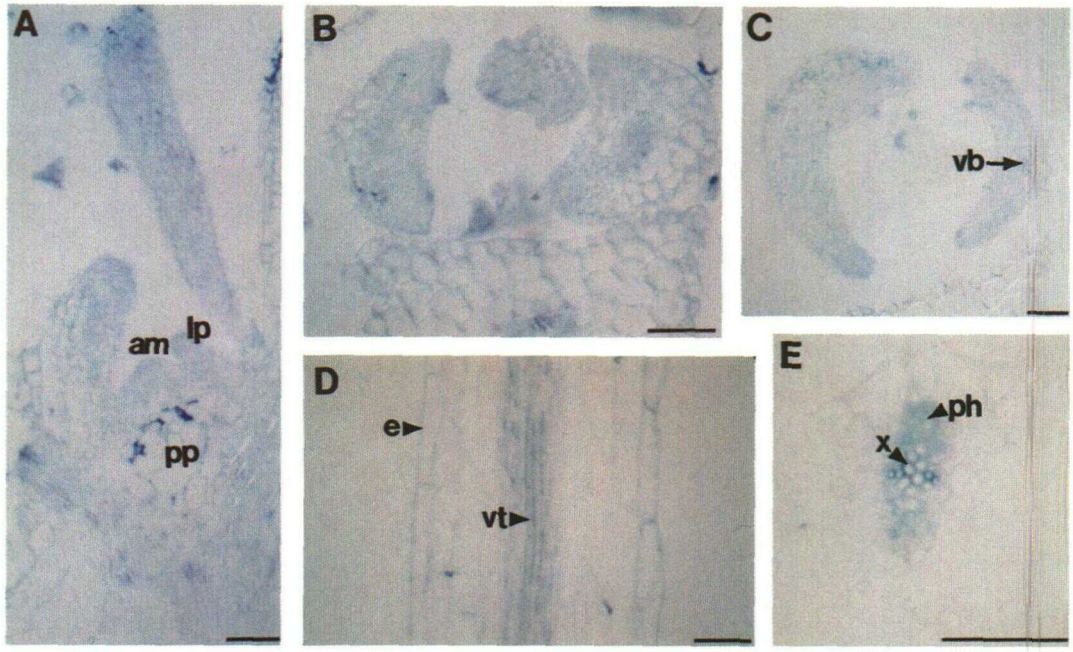

Figure 5. A, Shoot apex (longitudinal section). XETs were in the apical meristem and vascular tissue and in between pith parenchyma cells. Moderate, uniform levels of XETs were found within leaf primordia; however, there was a dramatic reduction of XET accumulation between cell layers in comparison with unstimulated plants. B and C, Leaf primordia and young developing leaves (transections). Meristematic cells with small vacuoles had moderate levels of XETs. A significant decrease in XET levels was found between cell layers. D, Hypocotyl (longitudinal section). XETs were in the vascular tissue and, in contrast to unstimulated plants, in the epidermis. E, Hypocotyl (transection). XETs were detected in abundance between vessels. am, Apical meristem; e, epidermis; lp, leaf primordium; ph, phloem; pp, pith parenchyma; vb, vascular bundle; vt, vascular tissue; x, xylem. Bars = 100 μm.

In addition to expanding cell walls, walls of cells experiencing mechanical strain may also be expected to require incorporation and cross-linking modifications of xyloglucan polymers to reinforce the walls under stress. The Arabidopsis XETs are found in the epidermal layers of cells at the attachment points of leaf and cotyledon petioles (Figs. 2I and 3L) and in hypocotyls subjected to wind (Fig. 5D). These results suggest that, because of the weight of a branching structure or movement accentuated by wind, XETs accumulate in the epidermis of the tissues under mechanical strain. XET activity may therefore contribute to strengthening the walls of tissues to prevent or limit mechanically induced cell and tissue damage. XET accumulation at these sites is consistent with the regulatory behavior of the *TCH4* gene, i.e. expression of *TCH4* is strongly up-regulated in plants subjected to mechanical perturbation (Braam and Davis, 1990; Xu et al., 1995). Regulation of *TCH3* is similar to that of *TCH4*, and the calmodulin-related TCH3 protein also accumulates at branch points (Sistrunk et al., 1994; Antosiewicz et al., 1995). Hypocotyl flexing or weight of a branching structure may provide a strain sufficient to lead to increases of the free cytosolic $[Ca^{2+}]$. $[Ca^{2+}]$ fluxes, probably within the epidermis, have been detected following wind and touch in plants (Knight et al., 1991, 1992), and increases in $[Ca^{2+}]$ may be necessary (Polisensky and Braam, 1996) and sufficient (Braam, 1992) to regulate *TCH* gene expression.

XETs may also aid in wall modifications required for the formation of xylem- and phloem-conducting elements. We found that XETs are in procambial strands (Fig. 2C), in differentiating vascular elements (Fig. 2, E–G), and in living elements of mature vascular tissue (Figs. 2H, 3L, and 4C). Following mechanical stimulation of plants, XET levels increase between vessels of hypocotyls (Fig. 5D), likely within the unlignified middle lamella of the primary xylem. Mechanostimulus-induced increases in strength or flexibility are often correlated with modification to the vascular tissue (Biddington, 1986; Telewski and Jaffe, 1986a, 1986b; Jaffe and Forbes, 1993; Mitchell and Myers, 1995). Therefore, a greater abundance of XETs at these locations may reflect a direct role for these enzymes in wall modification of vascular tissue, leading to the adaptive, developmental changes of thigmomorphogenesis. Because both the breakdown and biogenesis of walls contribute to the process of vascular differentiation and, because it is feasible to imagine that the enzymatic activity of an XET could contribute to either of these processes, it is difficult at this time to ascribe a mechanistic role for XET activity in vascular tissue differentiation.

The greatest concentration of XETs occurs asymmetrically around cells, either between adjacent cell layers or at corners where multiple cells come into contact (Figs. 2B and 3, C and F). Meristematic cells that will differentiate into spongy and palisade parenchyma elongate equally on both sides; however, XETs are not uniformly distributed around the expanding cells. Thus, the correlation between XET accumulation and cell expansion is weakened. The regions of greatest XET levels are places where intercellular

spaces or airspaces will form (Fig. 3, H and I). XET accumulation at these sites, therefore, may reflect a role for XET in intercellular space formation rather than cell expansion. The formation of intercellular spaces requires pectin solubilization, which leads to the dissolution of the middle lamella (Esau, 1977; Brett and Waldron, 1990). Polygalacturonase and β-galactosidase are thought to play key roles in pectin solubilization (Brett and Waldron, 1990; Redgwell et al., 1992). A requirement for XET function has not yet been assessed. XET activity may increase accessibility of the other cell wall enzymes by reducing the frequency of xyloglucan-cellulose microfibril cross-links. A similar activity for XETs has been proposed to be important for fruit ripening (Redgwell and Fry, 1993). Alternatively, because xyloglucan is found within intercellular spaces (K. VandenBosch and J. Braam, unpublished results), it is possible that xyloglucan and the action of XETs function to maintain the integrity of the tissue containing intercellular airspaces. XETs could enhance or rearrange xyloglucan cross-links to ensure sufficient cell-cell connections.

A maize XET-related protein has also been implicated in airspace formation. The *1005* gene was identified as a consequence of its up-regulation of expression in plants subjected to flooding and shows high sequence identity to known *XET* genes (Peschke and Sachs, 1994; Saab and Sachs, 1995). Expression of *1005* closely correlates with the early steps in the lysis of cortical tissue cells and airspace formation to generate aerenchyma in the root and mesocotyl (Saab and Sachs, 1996).

We also found that immunoreactive XETs are extremely abundant within single parenchyma cells that are located near the vascular bundles of leaves. This specific localization indicates that this cell must be distinct from its neighbors in properties and/or function. Cells that carry out polar auxin transport are expected to be in this region (Morris and Thomas, 1978; Jacobs and Gilbert, 1983); therefore, one possibility is that XETs specifically accumulate in cells conducting polar auxin transport. This pattern of protein accumulation may reflect the up-regulation of *TCH4* expression by low levels of exogenous IAA, a natural plant auxin (Xu et al., 1995, 1996).

In summary, TCH4 and possibly closely related XETs of Arabidopsis accumulate in specific regions during development. The pattern of localization coincides with regions of growth and cell wall modifications. We favor the hypothesis that TCH4, and XETs in general, functions in xyloglucan incorporation for reinforcement of cell walls during growth and in response to mechanical strain. In addition, XET action near certain cell types may contribute to partial wall lysis to allow formation of intercellular airspaces, tracheary elements, and sieve tubes. The choice between wall genesis and lysis may be determined by the types of xyloglucan substitutions present in the different tissue types. For example, *Zinnia* sp. mesophyll tissues have little or no fucosylated xyloglucan, whereas the epidermis and vascular tissue xyloglucan is more frequently fucosylated (McCann and Roberts, 1994). Alternatively, the different XET-related proteins may possess distinct enzymatic properties, such that an XET localized in cell corners serves to break xyloglucan connections, whereas an XET in the epidermis may function to tighten the wall by shortening xyloglucan-cellulose microfibril cross-links. Finally, the changes in XET localization in plants subjected to wind provide evidence that the XET's function may contribute to the physiological and morphogenetic alterations that enable plants to adapt to mechanical stresses of the environment.

ACKNOWLEDGMENT

We thank members of the Braam laboratory for critical reading of the manuscript.

Received June 20, 1997; accepted August 24, 1997.

LITERATURE CITED

Antosiewicz DM, Polisensky DH, Braam J (1995) Cellular localization of the Ca^{2+}-binding TCH3 protein of *Arabidopsis*. Plant J **8:** 623–636

Biddington NL (1986) The effects of mechanically-induced stress in plants—a review. Plant Growth Regul **4:** 103–123

Braam J (1992) Regulated expression of the calmodulin-related *TCH* genes in cultured *Arabidopsis* cells: induction by calcium and heat shock. Proc Natl Acad Sci USA **89:** 3213–3216

Braam J, Davis RW (1990) Rain-, wind-, and touch-induced expression of calmodulin and calmodulin-related genes in *Arabidopsis*. Cell **60:** 357–364

Braam J, Sistrunk ML, Polisensky DH, Xu W, Purugganan MM, Antosiewicz DM, Campbell P, Johnson KA (1996) Life in a changing world: *TCH* gene regulation of expression and responses to environmental signals. Physiol Planta **98:** 909–916

Brett C, Waldron K (1990) Physiology and Biochemistry of Plant Cell Walls. Unwin Hyman, London, pp 168–179

Carpita NC, Gibeaut DM (1993) Structural models of primary cell walls in flowering plants: consistency of molecular structure with the physical properties of the walls during growth. Plant J **3:** 1–30

Edelmann HG, Fry SC (1992) Effect of cellulose synthesis inhibition on growth and the integration of xyloglucan into pea internode cell walls. Plant Physiol **100:** 993–997

Esau L (1977) Anatomy of Seed Plants. John Wiley & Sons, New York, pp 48–49

Fanutti C, Gidley MJ, Reid JSG (1993) Action of a pure xyloglucan *endo*-transglycosylase (formerly called xyloglucan-specific *endo*-(1–4)-β-D-glucanase) from the cotyledons of germinated nasturtium seeds. Plant J **3:** 691–700

Farkas V, Sulova Z, Stratilova E, Hanna R, Maclachlan G (1992) Cleavage of xyloglucan by nasturtium seed xyloglucanase and transglycosylation to xyloglucan subunit oligosaccharides. Arch Biochem Biophys **298:** 365–370

Fry SC (1989) Cellulases, hemicelluloses and auxin-stimulated growth: a possible relationship. Physiol Plant **75:** 532–536

Fry SC, Smith RC, Renwick KF, Martin DJ, Hodge SK, Matthews KJ (1992) Xyloglucan endotransglycosylase, a new wall-loosening enzyme activity from plants. Biochem J **282:** 821–828

Hayashi T (1989) Xyloglucans in the primary cell wall. Annu Rev Plant Physiol Plant Mol Biol **40:** 139–168

Hayashi T, Marsden MPF, Delmer DP (1987) Pea xyloglucan and cellulose. V. Xyloglucan-cellulose interactions *in vitro* and *in vivo*. Plant Physiol **83:** 384–389

Hayashi T, Ogawa K, Mitsuishi Y (1994a) Characterization of the adsorption of xyloglucan to cellulose. Plant Cell Physiol **35:** 1199–1205

Hayashi T, Takeda T, Ogawa K, Mitsuishi Y (1994b) Effects of the degree of polymerization on the binding of xyloglucans to cellulose. Plant Cell Physiol **35:** 893–899

Hetherington PR, Fry SC (1993) Xyloglucan endotransglycosylase activity in carrot cell suspension during cell elongation and somatic embryogenesis. Plant Physiol **103:** 987–992

Jacobs M, Gilbert SF (1983) Basal localization of the presumptive auxin transport carrier in pea stem cells. Science **220:** 1297–1300

Jaffe MJ, Forbes J (1993) Thigmomorphogenesis: the effect of mechanical perturbation on plants. Plant Growth Regul **12:** 313–324

Knight MR, Campbell AK, Smith SM, Trewavas AJ (1991) Transgenic plant aequorin reports the effects of touch and cold-shock and elicitors on cytoplasmic calcium. Nature **352:** 524–526

Knight MR, Smith SM, Trewavas AJ (1992) Wind-induced plant motion immediately increases cytosolic calcium. Proc Natl Acad Sci USA **89:** 4967–4971

McCann MC, Roberts K (1994) Changes in cell wall architecture during cell elongation. J Exp Bot **45:** 1683–1691

McCann MC, Wells B, Roberts K (1990) Direct visualization of cross-links in the primary plant cell wall. J Cell Sci **96:** 323–334

Medford JI, Elmer J, Klee HJ (1991) Molecular cloning and characterization of genes expressed in shoot apical meristems. Plant Cell **3:** 359–370

Mitchell CA, Myers PN (1995) Mechanical stress regulation of plant growth and development. Hortic Rev **17:** 1–42

Morris DA, Thomas AG (1978) A microautoradiographic study of auxin transport in the stem of intact pea seedlings (*Pisum sativum* L.) J Exp Bot **29:** 147–157

Nishitani K (1995) Endo-xyloglucan transferase, a new class of transferase involved in cell wall construction. J Plant Res **108:** 137–148

Nishitani K, Tominaga R (1992) Endo-xyloglucan transferase, a novel class of glycosyltransferase that catalyzes transfer of a segment of xyloglucan molecule to another xyloglucan molecule. J Biol Chem **267:** 21058–21064

Norenburg JL, Barrett JM (1987) Steedman's polyester wax embedment and de-embedment for combined light and scanning electron microscopy. J Electron Microsc Technol **6:** 35–41

Okazawa K, Sato Y, Nakagawa T, Asada K, Kato I, Tomita E, Nishitani K (1993) Molecular cloning and cDNA sequencing of endoxyloglucan transferase, a novel class of glycosyltransferase that mediates molecular grafting between matrix polysaccharides in plant cell walls. J Biol Chem **34:** 25364–25368

Passioura JB, Fry SC (1992) Turgor and cell expansion: beyond the Lockhart equation. Aust J Plant Physiol **19:** 565–576

Peschke VM, Sachs MM (1994) Characterization and expression of anaerobically induced maize transcripts. Plant Physiol **104:** 387–394

Polisensky DH, Braam J (1996) Cold-shock regulation of the *Arabidopsis TCH* genes and the effects of modulating intracellular calcium levels. Plant Physiol **111:** 1271–1279

Potter I, Fry SC (1994) Changes in xyloglucan endotransglycosylase (XET) activity during hormone-induced growth in lettuce and cucumber hypocotyls and spinach cell suspension cultures. J Exp Bot **45:** 1281–1289

Pritchard J, Hetherington PR, Fry SC, Tomos AD (1993) Xyloglucan endotransglycosylase activity, microfibril orientation and the profiles of cell wall properties along growing regions of maize roots. J Exp Bot **44:** 1281–1289

Purugganan MM, Braam J, Fry SC (1997) The Arabidopsis TCH4 xyloglucan endotransglycosylase. Substrate specificity, pH optimum, and cold tolerance. Plant Physiol **115:** 181–190

Redgwell RJ, Fry SC (1993) Xyloglucan endotransglycosylase activity increases during kiwifruit (*Actinidia deliciosa*) ripening. Plant Physiol **103:** 1399–1406

Redgwell RJ, Melton LD, Brasch DJ (1992) Cell wall dissolution in ripening kiwifruit (*Actinidia deliciosa*). Solubilization of the pectic polymers. Plant Physiol **98:** 71–81

Saab IN, Sachs MM (1995) Complete cDNA and genomic sequence encoding a flooding-responsive gene from maize (*Zea mays* L.) homologous to xyloglucan *endo*transglycosylase. Plant Physiol **108:** 439–440

Saab IN, Sachs MM (1996) A flooding-induced xyloglucan *endo*transglycosylase homolog in maize is responsive to ethylene and associated with aerenchyma. Plant Physiol **112:** 385–391

Sistrunk ML, Antosiewicz DM, Purugganan MM, Braam J (1994) Arabidopsis *TCH3* encodes a novel Ca^{2+} binding protein and shows environmentally induced and tissue-specific regulation. Plant Cell **6:** 1553–1565

Smith RC, Fry SC (1991) Endotransglycosylation of xyloglucans in plant cell suspension cultures. Biochem J **279:** 529–535

Talbott LD, Ray PM (1992) Changes in molecular size of previously deposited and newly synthesized pea cell wall matrix polysaccharides. Effects of auxin and turgor. Plant Physiol **98:** 369–379

Telewski FW, Jaffe MJ (1986a) Thigmomorphogenesis: field and laboratory studies of *Abies fraseri* in response to wind or mechanical perturbation. Physiol Plant **66:** 211–218

Telewski FW, Jaffe MJ (1986b) Thigmomorphogenesis: anatomical, morphological and mechanical analysis of genetically different sibs of *Pinus taeda* in response to mechanical perturbation. Physiol Planta **66:** 219–226

Xu W, Campbell P, Vargheese AK, Braam J (1996) The *Arabidopsis XET*-related gene family: environmental and hormonal regulation of expression. Plant J **9:** 879–889

Xu W, Purugganan MM, Polisensky DH, Antosiewicz DM, Fry SC, Braam J (1995) *Arabidopsis TCH4*, regulated by hormones and the environment, encodes a xyloglucan endotransglycosylase. Plant Cell **7:** 1555–1567

Zurek DM, Clouse SD (1994) Molecular cloning and characterization of a brassinosteroid-regulated gene from elongating soybean (*Glycine max* L.) epicotyls. Plant Physiol **104:** 161–170